

Organic Acid-Based Natural Deep Eutectic Solvents: A Comparative Study for Chitin Extraction from Crab Shell By-Products

Nareerat Sunton^{1,2}, Chakkapat Anglong³, Maruj Limpawattana⁴, Wen-Can Huang¹,
Xiangzhao Mao¹ and Wanwimol Klaypradit^{2*}

ABSTRACT

Conventional chitin extraction using acid/alkali method is effective but involves harsh chemicals. Biological methods offer improved consistency but often result in limited chitin solubility. This study evaluated the efficiency of lactic acid-based and succinic acid-based natural deep eutectic solvents (NADES) for chitin extraction from crab shells. Choline chloride was mixed with either lactic acid (lactic-NADES) or succinic acid (succinic-NADES) and combined with crab shell powder (CS) in a 10:1 ratio. The mixture was then heated using microwaves for varying durations. The results showed that lactic-NADES achieved higher demineralization and deproteinization efficiencies than succinic-NADES. Optimal extraction was achieved with 3 M lactic acid at a CS: lactic-NADES ratio of 1:20, with a microwave irradiation time of 5 min, yielding demineralization and deproteinization efficiencies of $97.78 \pm 0.73\%$ and $81.33 \pm 0.91\%$, respectively. The microstructure, crystallographic organization, functional groups, and thermal stability of the optimal extracted chitin were then compared to those of conventionally extracted chitin. Analysis using SEM, FT-IR, XRD, and TGA showed that chitin obtained via the lactic-NADES method had characteristics comparable to those extracted using traditional acid/alkali methods. Thus, the lactic-NADES method presents a promising alternative for chitin extraction, offering similar quality with potentially fewer environmental impacts.

Keywords: Crustacean shells, Extraction of chitin, Lactic acid, NADES

INTRODUCTION

Chitin, a natural polysaccharide abundantly found in crustacean exoskeletons like crab shells (CS) (Joseph *et al.*, 2021), is a promising and sustainable resource for various industrial applications (Tolesa *et al.*, 2019). The extraction of chitin from CS is crucial for harnessing its potential, as it isolates the biopolymer from proteins and minerals. Traditionally, chitin extraction is achieved using conventional acid/alkali methods, which effectively remove non-chitin constituents but

involve harsh chemicals and generate significant waste (Aranaz *et al.*, 2009; Kumari and Kishor, 2020). An alternative approach involves biological extraction methods which produce chitin with improved consistency. However, these methods often result in limited chitin solubility and have their own constraints. Microbial extraction, an environmentally friendly method, has garnered significant interest. Researchers have explored various techniques for extracting chitin from crustacean shells, including fermentation, enzymatic processes, ionic liquids, and natural deep eutectic

¹College of Food science and Engineering, Ocean University of China, Shandong, China

²Department of Fishery products, Faculty of Fisheries, Kasetsart University, Bangkok, Thailand

³Department of Animal Science, Faculty of Agriculture at Kamphaeng Saen, Kasetsart University, Kamphaeng Saen Campus, Nakhon Pathom, Thailand

⁴Department of Food Technology, Faculty of Science, Siam University, Bangkok, Thailand

*Corresponding author. E-mail address: ffiswak@ku.ac.th

Received 10 June 2024 / Accepted 18 November 2024

solvents (NADES) (Hamed *et al.*, 2016; Pachapur *et al.*, 2016; Liu *et al.*, 2018; Kumari and Kishor, 2020; Joseph *et al.*, 2021).

NADES, made from natural eutectic compounds based on acids, organic carbon sources, and choline-chloride (Dai *et al.*, 2013b), have emerged as eco-friendly and milder alternatives for chitin extraction. They offer several advantages over conventional extraction methods, including reduced environmental impact, biodegradability, and customizable solvent composition (Saravana *et al.*, 2018). Previous studies (Liu *et al.*, 2018; Santana *et al.*, 2019) have shown that NADES provide a more sustainable and efficient method for chitin extraction compared to traditional acid/alkali methods. NADES- extracted chitin has demonstrated improved crystallinity and thermal stability (El Knidri *et al.*, 2018). Additionally, NADES have been reviewed for their applications in extraction, enzymatic reactions, solubility enhancement, and as media for pharmaceuticals and cosmetics Vanda *et al.* (2018).

Mineral and protein removal is critical for chitin and chitosan production. NADES offer a promising deproteinization alternative due to their environmentally friendly nature and low toxicity (Saravana *et al.*, 2018; Vicente *et al.*, 2021), making them particularly beneficial for food manufacturers aiming to enhance the purity of chitin or chitosan for functional ingredients or additives (Shamshina *et al.*, 2019).

Lactic acid and succinic acid are key organic acids used in this study. Lactic acid, known for its higher acidity due to the presence of a hydroxyl group adjacent to the carboxyl group, is widely used in organic synthesis and biochemical industries. Succinic acid, a dicarboxylic acid obtained from natural sources, finds applications in drug compounds, agriculture, food production, and industry (Saxena *et al.*, 2017). Previous study (Gómez *et al.*, 2019) has investigated the polymerization of mixtures of choline chloride with lactic acid or succinic acid to determine the ratios that influence polymer reactions.

To enhance chitin extraction, methods such as heating, agitating, ultrasound, and microwave-assisted synthesis are employed (Santana *et al.*, 2019). Microwave-assisted extraction, which involves irradiating substances in a controlled system, enhances heat distribution and accelerates reactions, reducing energy consumption and processing time compared to traditional methods (Gomez *et al.*, 2018).

This study aimed to determine the demineralization and deproteinization efficiency of lactic acid-based and succinic acid-based NADES for chitin extraction from crab shells. Additionally, chitin extracted under optimal condition using NADES and microwave-assisted extraction was compared to conventionally extracted chitin in terms of demineralization and deproteinization efficiency, morphology using scanning electron microscopy (SEM), functional groups using fourier-transform infrared (FT-IR), crystal structure using X-ray diffraction (XRD), and thermogravimetric analysis (TGA).

MATERIALS AND METHODS

Preparation of natural deep eutectic solvent (NADES)

NADES were prepared following the method described by Gontrani *et al.* (2019) and Yang (2019), with slight modifications. In this study, a novel NADES was synthesized using 1 M of choline chloride (ChCl), a quaternary ammonium salt, as the hydrogen bond donor, and lactic acid (LA) or succinic acid (SA) as the hydrogen bond acceptor, both at a concentration of 1 M. The two reagents were thoroughly mixed, and then heated and stirred at 80 °C for 10 min until a homogenous solution was formed. The resulting NADES were transferred to an amber glass bottle and stored at 4 °C for further analysis. Lactic-NADES were specifically prepared by mixing ChCl with LA at various concentrations (1 M, 2 M, and 3 M) to be used as NADES for subsequent experiments.

Preparation of chitin from crab shell

Crab (*Portunus pelagicus*) shells (CS) collected from Chonburi Province, Thailand, were cleaned and dried in a hot air oven at 105 °C for 12 h. To obtain CS powder, the dried shells were ground using a high-speed blender and passed through a 60-mesh sieve. The resulting CS powder was then subjected to two different chitin extraction methods: NADES method and the conventional acid/alkaline method, which served as the control.

For the NADES method, CS was individually extracted using either lactic-NADES or succinic-NADES at a 1:10 w/v ratio, with microwave irradiation times of 5, 10, 15, and 20 min to determine the optimal organic acid for chitin extraction. Lactic-NADES was further tested by mixing CS with lactic acid at varying ratios (1:10, 1:15, and 1:20 w/v) and subjected to microwave irradiation for 5, 10, or 15 min. The mixtures were heated in a microwave oven at 700 W for the specified durations. After heating, the mixtures were centrifuged at 8,000 × g for 15 min at 25 °C. The resulting sediment, referred to as extracted NADES chitin, was washed with deionized water and subsequently dried using a hot air oven at 70 °C for 6 h.

For the conventional acid/alkali method, following Shamshina *et al.* (2019) with slight modification, CS was mixed with 1 M HCl at a 1:10 w/v ratio to dissolve minerals, and continuously stirred at ambient temperature for 12 h. Subsequently, the mixture was centrifuged at 8,000 × g for 15 min at 25 °C, and the demineralized CS was washed with deionized water until the pH reached 7. Next, the demineralized CS was mixed with 2 M NaOH at a 1:20 w/v ratio to remove proteins, and stirred at ambient temperature for another 12 h. After centrifugation at 8,000 × g for 15 min at 25 °C, the sediment, known as extracted conventional acid/alkali chitin, was washed with deionized water and dried in a hot air oven at 70 °C for 6 h. All extracted chitin samples were stored in amber glass bottles in a desiccator at ambient temperature until further analysis.

Characterization of extracted chitin: a comparative physical and chemical analysis between NADES and acid-alkaline methods

Demineralization efficiency

The NADES chitin and acid/alkali chitin samples were subjected to heat treatment in a furnace (Nabertherm P330, Germany) at 550 °C for 5 h. Subsequently, the demineralization efficiency was calculated using equation (1).

$$\text{Demineralization efficiency (\%)} = [(W_1 - W_2)/W_1] \times 100 \quad (1)$$

Where W_1 is the weight of the ash content in CS (g) and W_2 is the weight of the ash content in NADES chitin or acid/alkali chitin (g).

Deproteinization efficiency

The protein content of NADES chitin and acid/alkali chitin were determined using the Bradford protein assay (Pedrol and Tamayo, 2001). Deproteinization efficiency was calculated using equation (2).

$$\text{Deproteinization efficiency (\%)} = [(P_1 - P_2)/P_1] \times 100 \quad (2)$$

Where P_1 is the protein content in CS and P_2 is the protein content in NADES chitin or acid/alkali chitin.

Scanning electron microscope (SEM)

The morphology of the samples were examined using a scanning electron microscope (SEM) (Quanta 250 FEG, FEI, USA) operating in secondary electron mode at an accelerating voltage of 10 kV. The samples were freeze-dried and mounted on aluminum stubs with conductive carbon tape. Subsequently, a thin platinum film was sputter-coated onto the samples to enhance image resolution and minimize charging effects during imaging. The morphology was observed at 5,000× magnification.

Fourier transform infrared spectroscopy (FT-IR)

The Fourier transform infrared spectroscopy (FT-IR) spectra of the samples were analyzed using an FT-IR spectrometer (Invenio S, Bruker, USA) at room temperature. The measurement range covered 4,000–400 cm⁻¹ (mid-IR region). Signals were collected automatically and analyzed using the OPUS 3.0 software (Bruker).

X-ray diffraction (XRD)

The crystal structure and phase composition of the samples were analyzed using an X-ray diffractometer (D8 Advance, Bruker, Germany) with Cu K- α radiation ($\lambda = 1.54056$ nm). Scanning was conducted over a 2 θ range of 5° to 60° with step increments of 5° min⁻¹. The X-ray diffractometer operated at 40 kV and 40 mA, following JCPDS card number 05-0586.

Thermogravimetric analysis (TGA)

Thermal degradation of the samples were analyzed using a Thermogravimetric Analyzer (NETZSCH, Germany). Samples were heated under a nitrogen atmosphere from 30 to 900 °C at a rate of 10 °C·min⁻¹. This allowed us to study the weight changes and thermal stability of the samples under controlled conditions.

Statistical analysis

Data were collected in triplicate and are presented as mean \pm standard deviation (SD). To assess statistical significance between means of three or more groups, a one-way analysis of variance (ANOVA) was employed. Mean comparisons were performed using Duncan's Multiple Range Test with significance considered at $p < 0.05$. All statistical analyses were conducted using the SPSS package (SPSS for Windows, Inc., Chicago, IL, USA).

RESULTS AND DISCUSSION

Comparative analysis of demineralization and deproteinization efficiency: lactic-NADES and succinic-NADES

Demineralization efficiency

Demineralization efficiency refers to the removal of mineral components, primarily calcium carbonate, from the crab shell matrix, leaving behind the chitin-rich fraction (Ozel and Elibol, 2021). As shown in Figure 1, the demineralized efficiency of chitin extraction from CS using lactic- and succinic-NADES at a 1:10 w/v ratio was thoroughly investigated across various microwave irradiation times (5, 10, 15, and 20 min). The results revealed distinct differences in the performance of the two acids, highlighting their respective capabilities in the extraction process. Lactic-NADES consistently yielded higher demineralized efficiency compared to succinic-NADES at all time points ($p < 0.05$). Additionally, the results indicated that longer microwave irradiation times improved the demineralization efficiency for both lactic- and succinic-NADES, suggesting that extended irradiation allows for more effective mineral removal and leading to enhanced chitin yield for both acids.

The superiority of lactic-NADES over succinic-NADES in chitin extraction can be attributed to several factors. Firstly, lactic acid may have a greater capacity to dissolve the mineral components of the crab shell, leading to more efficient demineralization and higher chitin yield. Furthermore, the chemical structure of lactic-NADES might exhibit a stronger affinity for chitin, facilitating its extraction. These findings are consistent with previous research which highlights the influence of different solvents on the efficiency of chitin extraction from crustacean shells (Yang, 2019).

Deproteinization efficiency

The deproteinization efficiency of lactic- and succinic-NADES during chitin extraction from CS was investigated at various microwave irradiation times (5, 10, 15, and 20 min), as shown in Figure 2.

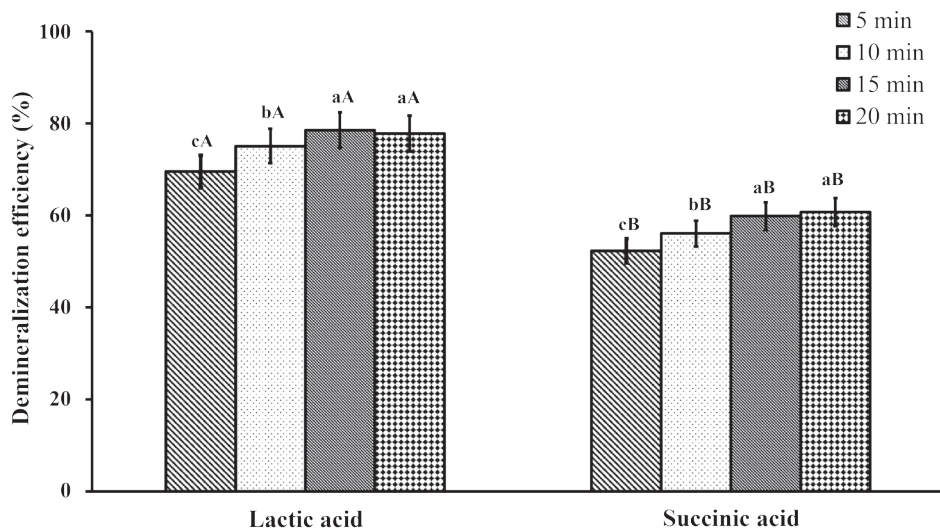


Figure 1. Demineralization efficiency of lactic- and succinic-NADES in chitin extraction from crab shells (CS) at 5, 10, 15, and 20 min. Bars and error bars represent mean values ($n = 3$) and SD, respectively. Different lowercase letters above bars indicate significant differences between microwave irradiation time ($p < 0.05$), while different uppercase letters indicate significant differences between the acids ($p < 0.05$) within the same duration.

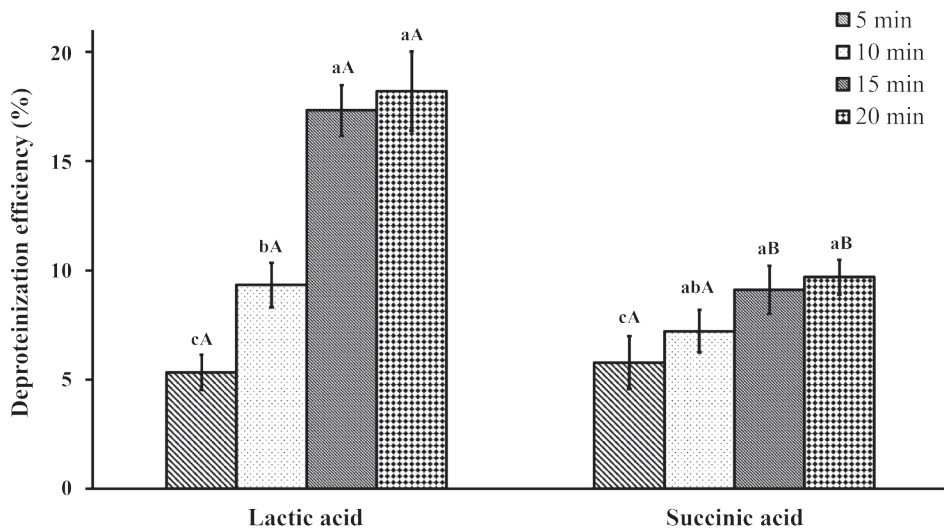


Figure 2. Deproteinization efficiency of lactic- and succinic-NADES in chitin extraction from crab shells (CS) at 5, 10, 15, and 20 min. Bars and error bars represent mean values ($n = 3$) and SD, respectively. Different lowercase letters above bars indicate significant differences between microwave irradiation times ($p < 0.05$), while different uppercase letters indicate significant differences between the acids ($p < 0.05$) within the same duration.

The results revealed distinct differences in deproteinization efficiency between the two acids, with lactic-NADES consistently exhibiting superior efficiency compared to succinic-NADES at all time points. This advantage may be attributed to the unique properties of lactic acid, such as its stronger acidity and better interaction with proteins. The protonation of amides, a rapid process in acidic conditions, effectively removes protein during extraction (Vicente *et al.*, 2021). The data also demonstrate the time-dependent nature of deproteinization. As microwave irradiation time increased, both lactic- and succinic-NADES exhibited improved deproteinization efficiency, indicating that longer irradiation allows the acids to interact more effectively with the protein components, leading to greater protein removal and higher deproteinization yields. These findings have important implications for chitin extraction applications. The superior deproteinization efficiency of lactic-NADES suggests its potential as a more efficient and effective deproteinizing agent in the chitin extraction process. Consequently, lactic-NADES shows promise for further study and application in processes requiring high demineralization and deproteinization efficiencies.

Optimizing chitin extraction with lactic-NADES: influence of lactic acid concentrations and crab shell to lactic-NADES ratios

Demineralization efficiency

The results of the demineralization efficiency using lactic-NADES at different molar concentrations (M) and CS: lactic-NADES ratios are presented in Table 1. The demineralization efficiency exhibited distinct patterns in response to variations in lactic acid concentration, CS: lactic-NADES ratio, and microwave irradiation time. The data clearly demonstrate a significant positive correlation between the molar concentration of lactic-NADES and their demineralization efficiency. As the molar concentration increased from 1 M to 3 M, a substantial improvement in demineralization efficiency was observed across all time intervals (5, 10, and 15 min). For instance, at 1 M, the demineralization efficiency increased from 69.54% at 5 min to 76.55% at 15 min. At 3 M, the efficiency ranged from 94.66% to 95.13%, indicating a statistically significant improvement compared to the other groups ($p<0.05$). The significant increase in efficiency with higher concentrations of lactic-

Table 1. Demineralization efficiency of lactic-NADES at various concentrations of lactic acid (1, 2, and 3 M) with different CS: lactic-NADES ratios (1:10, 1:15, and 1:20) in chitin extraction from crab shells (CS) at 5, 10, and 15 min of microwave irradiation time.

Lactic acid concentration (M)	CS: Lactic-NADES (w/v)	Demineralization efficiency (%)		
		Microwave irradiation time (min)		
		5	10	15
1	1:10	69.54±1.51 ^{cF}	75.11±0.85 ^{bF}	76.55±0.59 ^{aG}
	1:15	72.22±0.82 ^{cE}	77.48±0.24 ^{bE}	80.59±0.55 ^{aE}
	1:20	79.55±0.86 ^{cD}	85.56±0.75 ^{bD}	89.06±0.84 ^{aD}
2	1:10	72.85±0.95 ^{cE}	74.25±0.99 ^{bF}	78.46±0.89 ^{aF}
	1:15	99.20±0.56 ^{aA}	99.86±0.17 ^{aA}	98.81±0.69 ^{aA}
	1:20	98.94±0.58 ^{aAB}	98.02±0.28 ^{aB}	97.85±0.92 ^{aB}
3	1:10	94.66±0.35 ^{bC}	95.58±0.73 ^{aC}	95.13±0.45 ^{aC}
	1:15	99.82±0.12 ^{aA}	99.74±0.14 ^{aA}	99.79±0.11 ^{aA}
	1:20	97.78±0.73 ^{aB}	98.07±0.94 ^{aAB}	97.67±0.87 ^{aB}

Note: Values are presented as mean±SD (n = 3). Data were calculated on a dry weight basis. Different lowercase letters above means in the same row indicate significant difference ($p<0.05$); Different uppercase letters in the same column indicate significant difference ($p<0.05$).

NADES is consistent with established research (Dai *et al.*, 2013a; Paiva *et al.*, 2014; Vanda *et al.*, 2018). Elevated molar concentrations provide a greater pool of active demineralizing species, which accelerates the dissolution of mineral content from the enamel surface (Gómez *et al.*, 2019). These findings highlight the potential of lactic-NADES as effective demineralizing agents and warrant further investigation to optimize their concentration range for achieving maximal efficiency.

The findings also demonstrate a substantial impact of the CS: lactic-NADES ratio on the demineralization process within each group. The varying microwave irradiation times reveal the significance of solvent composition in regulating the effectiveness of lactic-NADES based demineralization. At a concentration of 1 M, the demineralization efficiency was highest at 89.06 ± 0.84 when using a mixture of CS and lactic-NADES in a 1:20 ratio at 15 min. This was superior to the efficiencies observed with lactic-NADES in 1:10 and 1:15 ratios. However, at concentrations of 2 M and 3 M, demineralization efficiency did not significantly differ ($p>0.05$) between CS and lactic-NADES ratios of 1:15 and 1:20, regardless of microwave irradiation time. When evaluating

demineralization efficiency at various lactic acid concentrations and ratios of CS and lactic-NADES while keeping the microwave irradiation time constant, the results indicated that demineralization efficiency generally increased, particularly when using lactic acid at 2 M and 3 M with ratios of 1:15 and 1:20, compared to using lactic acid at 1 M. The results of this study align with the previous research that highlights the importance of the composition of solvents in controlling the properties and functions of NADES (Liu *et al.*, 2018). Varying ratios of choline-based salts and lactic acid can lead to variations in the physicochemical properties of NADES, which, in turn, influence the diffusion rate of demineralizing agents and their interactions with the enamel surface (Ozel and Elibol, 2021). The findings offer avenues for further research and development in food processing to harness the full potential of these solvents for controlled demineralization and other innovative applications.

Deproteinization efficiency

The investigation into deproteinization efficiency using lactic-NADES at different molar concentrations, CS: lactic-NADES ratios, and microwave irradiation times is presented in Table 2.

Table 2. Deproteinization efficiency of lactic-NADES at various concentrations of lactic acid (1, 2, and 3 M) with different CS: lactic-NADES ratios (1:10, 1:15, and 1:20) in chitin extraction from crab shells (CS) at 5, 10, and 15 min of microwave irradiation time.

Lactic acid concentration (M)	CS: Lactic-NADES (w/v)	Demineralization efficiency (%)		
		5	10	15
1	1:10	5.33 \pm 0.72 ^{cl}	9.33 \pm 0.43 ^{bl}	17.33 \pm 0.89 ^{al}
	1:15	9.33 \pm 0.88 ^{ch}	20.27 \pm 1.01 ^{bh}	29.33 \pm 0.49 ^{ah}
	1:20	27.60 \pm 0.18 ^{ce}	29.33 \pm 0.73 ^{bf}	33.00 \pm 0.44 ^{af}
2	1:10	14.67 \pm 0.95 ^{cg}	26.07 \pm 0.61 ^{bg}	36.00 \pm 0.38 ^{ag}
	1:15	24.00 \pm 0.11 ^{cf}	38.00 \pm 0.73 ^{be}	40.00 \pm 1.11 ^{ae}
	1:20	56.40 \pm 0.72 ^{cd}	57.07 \pm 0.63 ^{bd}	58.67 \pm 0.77 ^{ad}
3	1:10	60.80 \pm 0.59 ^{cc}	72.00 \pm 0.55 ^{bc}	78.67 \pm 0.84 ^{ac}
	1:15	65.33 \pm 0.73 ^{cb}	75.47 \pm 0.77 ^{bb}	91.33 \pm 0.93 ^{ab}
	1:20	81.33 \pm 0.91 ^{ca}	90.53 \pm 0.48 ^{ba}	93.07 \pm 1.12 ^{aA}

Note: Values are presented as mean \pm SD ($n = 3$). Data were calculated on a dry weight basis. Different lowercase letters above means in the same row indicate significant difference ($p<0.05$); Different uppercase letters in the same column indicate significant difference ($p<0.05$).

The data reveal a clear correlation between higher lactic acid molar concentrations and increased deproteinization efficiency. Across various CS: lactic-NADES ratios and microwave irradiation times, deproteinization efficiency improved as the molar concentration of lactic acid increased. At the lowest concentration of 1 M, the efficiency ranged from 5.33% to 33.00%, while at the highest concentration of 3 M, the efficiency significantly increased, ranging from 60.80% to 93.07%. This finding is consistent with previous research by Saravana *et al.* (2018), who explored the application of NADES for bioactive compound extraction. Similarly, Liu *et al.* (2018) reported that higher lactic acid concentrations in NADES improved extraction yields due to enhanced solvent-solute interactions and solubility. The CS: lactic-NADES ratio also proved to be a significant determinant of deproteinization efficiency. Specifically, a ratio of 1:20 consistently demonstrated superior efficiency compared to ratios of 1:10 and 1:15, indicating that a higher concentration ratio is optimal for achieving greater protein removal (Gómez *et al.*, 2019). Optimizing the ratio between CS and lactic-NADES is, therefore, crucial for maximizing deproteinization efficiency.

Moreover, the data revealed a pronounced positive correlation between the duration of microwave irradiation times and deproteinization efficiency. Irrespective of molar concentration and CS: lactic-NADES ratio, efficiency consistently increased with longer microwave irradiation times. At the highest molar concentration of 3 M and a CS: lactic-NADES ratio of 1:20, the efficiency surged from 81.33% at 5 min to an impressive 93.07% at 15 min. These findings underscore the importance of allowing sufficient time for the deproteinization process to reach optimal efficacy. This observation aligns with related studies, such as Saravana *et al.* (2018), who found that prolonged extraction times led to enhanced yields due to the progressive dissolution of target compounds.

Based on the observed demineralization and deproteinization efficiencies during chitin extraction, the optimal conditions were determined to be 3 M lactic acid with a CS to lactic-NADES ratio of 1:20 and a microwave time of 5 min. Under

these conditions, a demineralization efficiency of $97.78 \pm 0.73\%$ and a deproteinization efficiency of $81.33 \pm 0.91\%$ were achieved. This condition was chosen because demineralization efficiency did not vary significantly with different microwave times ($p > 0.05$), and although deproteinization efficiency was lower than at 10 and 15 min, an efficiency of over 80% was considered acceptable.

Comparative characterization of crab shell chitin: traditional method and lactic-NADES method

Surface morphology of crab shells, chitin extracted using conventional acid/alkali, and chitin extracted using lactic-NADES

Based on the earlier results of demineralization and deproteinization efficiency using lactic-NADES at different molar concentrations and CS: lactic-NADES ratios, the optimized condition was found to be 3 M concentration of lactic-NADES with a CS: lactic-NADES ratio of 1:20 and microwave irradiation time of 5 min. This condition exhibited an impressive demineralization efficiency of $97.78 \pm 0.73\%$ and deproteinization efficiency of $81.33 \pm 0.91\%$. This optimized condition shows great promise for further study and potential applications in chitin extraction processes.

As shown in Figure 3, surface morphology images provide valuable visual insights into the microstructure of materials and play a vital role in assessing the quality and effectiveness of different extraction processes for obtaining chitin from CS. In Figure 3a, the SEM image of CS in powder form reveals irregularly shaped and fragmented particles. CS is composed mainly of chitin, a tough and rigid biopolymer. The surface of the particles displays a rough and granular texture due to the natural structure of the exoskeleton (Kumari and Kishor, 2020). Some parts of the particles appear smooth, while others are rough, depending on the extent of grinding. The particles also exhibit variation in size and shape, reflecting the heterogeneous nature of CS. In Figure 3b, the SEM image of chitin extracted using acid/alkali (AA-Ch) shows a more distinct and refined structure compared to the CS. The chitin extracted through acid and alkali treatment undergoes deproteinization and demineralization,

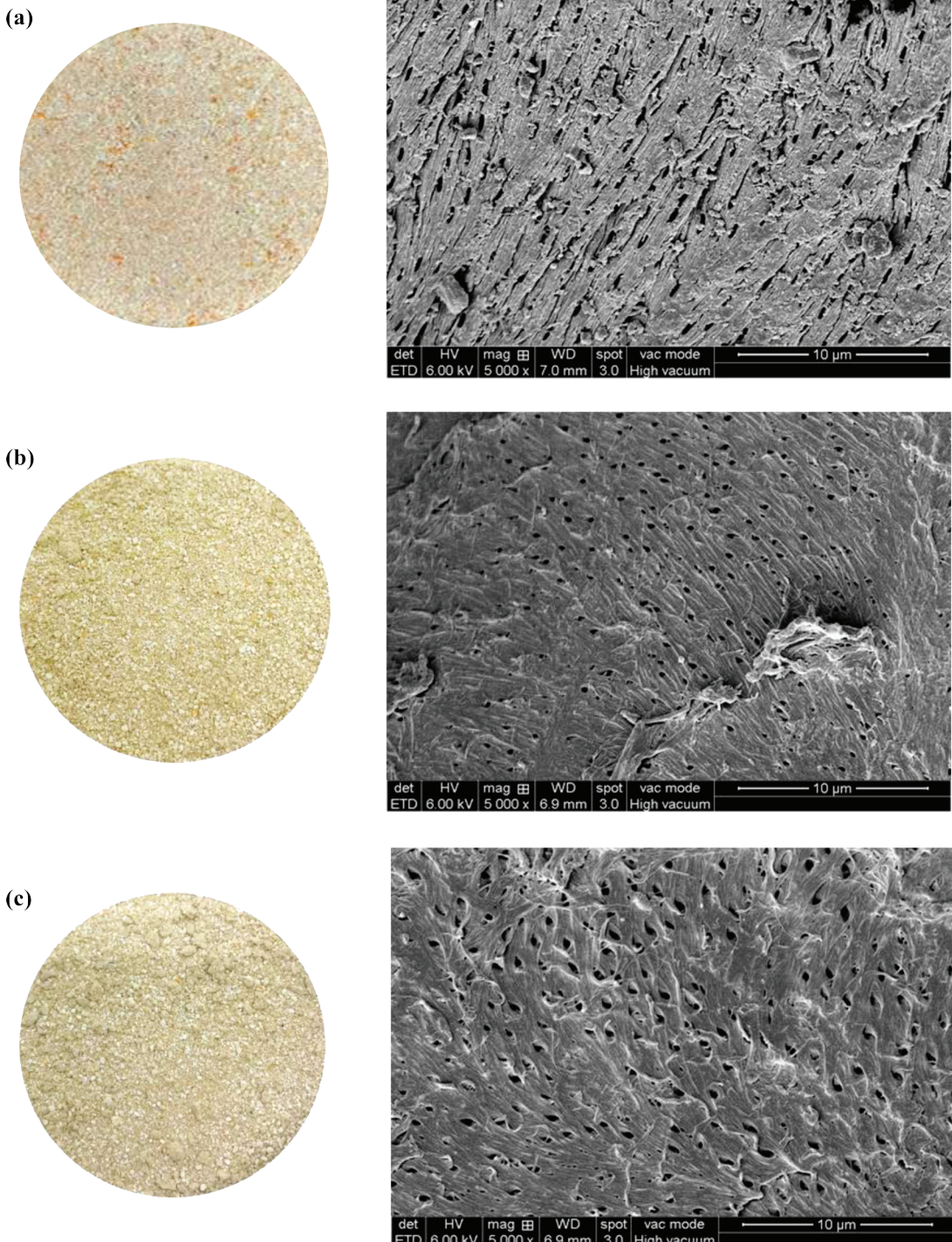


Figure 3. SEM images showing: (a) the morphology of crab shells powder (CS); (b) chitin extracted using acid/alkali (AA-Ch); and (c) chitin extracted using lactic-NADES (lactic-NADES chitin).

leading to the removal of proteins and minerals from CS. The resulting chitin appears more homogeneous and exhibits a fibrous or fibrillar structure. The surface also has a smoother appearance, with the fibers more organized and aligned. The SEM image also shows individual chitin fibers or aggregated structures, highlighting the purified and processed nature of the material. The SEM image of chitin extracted using lactic-NADES (Figure 3c) reveals distinct features comparable to those obtained through the conventional acid/alkali extraction method. NADES offer a greener and milder approach to deproteinization, potentially resulting in chitin with different properties (Paiva *et al.*, 2014; Liu *et al.*, 2018). The SEM image reveals a surface with a different texture or morphology compared to chitin extracted by conventional acid/alkali. Depending on the specific NADES formulation and extraction conditions, the chitin fibers exhibited a finer appearance and better alignment, indicating the potential of NADES as a greener and milder alternative for chitin extraction (Rahayu *et al.*, 2022). In a comparative study by Zhu *et al.* (2017), three different chitin extraction methods, including conventional acid/alkali treatment, enzymatic extraction, and lactic-NADES, were applied to CS. The SEM images of chitin

extracted via conventional acid/alkali treatment showed a fibrous structure with some irregularities. Interestingly, the chitin extracted using lactic-NADES displayed a finely fibrillar structure with improved alignment and uniformity, suggesting a distinct microstructure due to the unique properties of the solvent system.

X-ray diffraction (XRD)

X-ray diffraction (XRD) was employed to investigate the crystalline structure of CS and chitin extracted using different methods. The XRD patterns of CS, AA-Ch, and lactic-NADES are illustrated in Figure 4. In the XRD pattern of CS (Figure 4a), several diffraction peaks typically correspond to the natural crystalline structure of chitin, the main component of the exoskeleton. The pattern displays sharp peaks at characteristic angles, reflecting the crystalline nature of chitin in CS. Calcite and aragonite crystalline phases were also identified in powdered CS. According to JCPDS card number 05-0586, the calcite crystals in CS are denoted by peaks at 2θ : 29.404, 39.399, and 43.143. The presence of additional or broadened peaks may indicate other mineral phases, such as calcium carbonate, commonly found in CS. In the

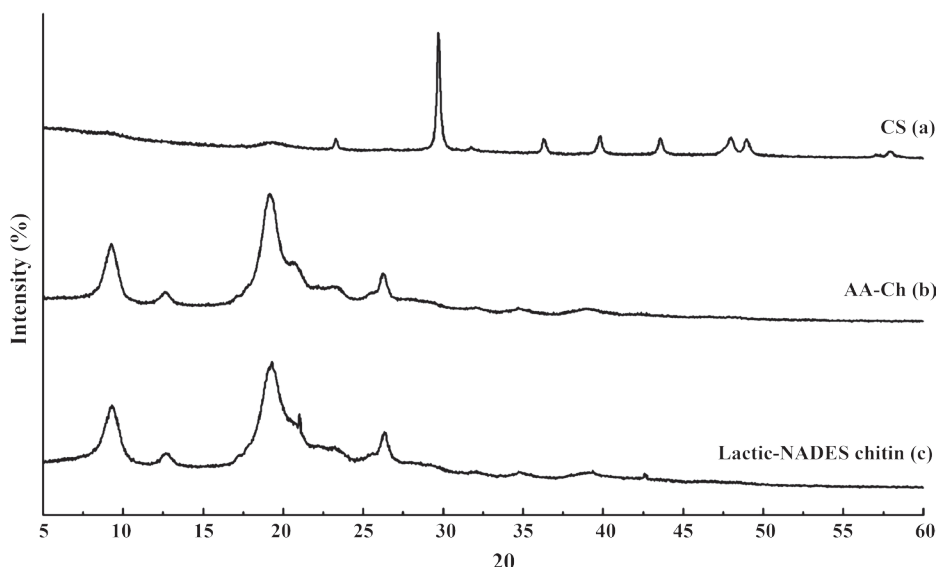


Figure 4. Figures showing XRD pattern of: (a) crab shells (CS) in powder form; (b) chitin extracted using acid/alkali (AA-Ch); and (c) chitin extracted using natural deep eutectic solvents (NADES) (lactic-NADES chitin).

XRD pattern of AA-Ch (Figure 4b), the peaks would correspond to the crystallographic planes of chitin, indicating the successful removal of impurities like proteins and minerals through acid/alkali treatment. The chitin-specific peaks show enhanced intensity, reflecting the high purity and concentration of the extracted chitin.

Similarly, the XRD pattern of chitin obtained from lactic-NADES (Figure 4c) is particularly interesting due to the distinctive extraction technique. This pattern may vary depending on the specific NADES formulation and extraction conditions, showing differences from the conventional acid/alkali extraction. While it resembles the AA-Ch pattern, indicating a similar crystalline structure, there may be fluctuations in peak intensities or minor shifts in peak positions due to the influence of lactic-NADES on the chitin structure. A comparative study by Li *et al.* (2023) used XRD to compare the crystallinity of chitin extracted from CS using conventional acid/alkali treatment and lactic-NADES. The XRD patterns revealed that chitin extracted via conventional acid/alkali treatment displayed well-defined peaks, while the lactic-NADES extracted chitin showed altered peak shapes and intensities. The chitin extracted using lactic-NADES exhibited a lower degree of crystallinity, suggesting potential structural modifications induced by the milder extraction conditions of lactic-NADES. In a study by Saravana *et al.* (2018), the influence of different lactic-NADES formulations on chitin crystallinity was investigated. XRD analysis revealed that chitin extracted using various lactic-NADES compositions exhibited distinct XRD patterns with variation in peak positions and intensities. These findings indicate that the specific lactic-NADES formulation influences the chitin crystalline structure, emphasizing the importance of tailoring the lactic-NADES composition to achieve desired chitin properties. Moreover, Saravana *et al.* (2018) also examined the effect of extraction time on the crystalline structure of chitin extracted using lactic-NADES. XRD analysis showed that the degree of crystallinity increased with prolonged extraction time. The XRD patterns exhibited sharper peaks with prolonged extraction, indicating enhanced chitin crystallinity due to prolonged interaction with the lactic-NADES.

FT-IR spectroscopy analysis

FT-IR spectroscopy is a powerful tool for characterizing the chemical composition and structural properties of chitin extracted from different sources using different methods (Pemberton *et al.*, 2018). FT-IR spectra provide valuable insights into the quality and purity of the extracted chitin, as well as any structural modifications induced by different extraction processes. This information helps researchers understand the effects of various extraction methods and solvents on the chitin structure and properties, ultimately contributing to the optimization of chitin extraction protocols for various applications. The FT-IR spectra of CS, AA-Ch, and chitin extracted from lactic-NADES are presented in Figure 5. In the FT-IR spectrum of CS (Figure 5a), several characteristic peaks corresponding to the functional groups present in the CS components were observed. Notably, absorption bands in the fingerprint region (around 1,000–1,500 cm⁻¹) correspond to the C-O and C-N stretching vibrations of chitin. The FT-IR spectrum of chitin exhibited characteristic peaks at around 1,650 cm⁻¹ (amide I band) and 1,560 cm⁻¹ (amide II band), indicative of the presence of chitin with its typical proteinaceous structure. For chitin extracted via conventional acid/alkali treatment, the amide I and amide II bands were observed at 1,630 and 1,554 cm⁻¹, respectively (Figure 5b). In contrast, chitin extracted using lactic-NADES showed these bands at 1,631 and 1,547 cm⁻¹, respectively (Figure 5c). Additionally, a broad band in the region around 3,000–3,600 cm⁻¹ corresponding to O-H stretching vibrations from hydroxyl groups, was evident in both the acid/alkali and lactic-NADES extracted chitin, (Figure 5b and 5c) at with absorption peaks at 3,261 and 3,258 cm⁻¹, respectively. This feature is typical in chitin and other organic components. In a study by Margariti (2019), FT-IR spectroscopy was employed to analyze chitin extracted from CS using conventional acid/alkali treatment. The spectrum exhibited characteristic absorption bands associated with chitin, although slight shifts in intensities were observed due to the influence of NADES on the chitin structure. Additionally, the spectrum showed strong absorption bands around 1,020 cm⁻¹ and 1,150 cm⁻¹, corresponding to C-O and C-N stretching

vibrations, respectively, further confirming the presence of chitin in the extracted sample. Moreover, in a comparative study by de Queiroz Antonino *et al.* (2017), FT-IR spectroscopy was utilized to compare the chitin extracted from CS using different methods, including conventional acid/alkali and enzymatic extraction. The FT-IR spectra revealed similar characteristic peaks related to the chitin structure in both extraction methods. However, slight variations in peak intensities indicated differences in the degree of deproteinization and the purity of the chitin obtained from each method. Similarly, Zhu *et al.* (2017) investigated the FT-IR spectrum of chitin extracted from CS using lactic-NADES. The FT-IR spectrum exhibited slight variations in peak positions compared to chitin extracted via conventional acid/alkali, suggesting potential structural differences induced by the NADES. Zhu *et al.* (2017) also explored the influence of different lactic-NADES formulations on the FT-IR spectra of chitin. The FT-IR analysis showed that the NADES-extracted chitin displayed distinctive peaks and variations in intensities compared to chitin extracted using conventional methods. These differences in the FT-IR spectra suggested structural modifications in the chitin, likely due to the specific composition of the NADES used in the extraction process.

TGA analysis

TGA analysis is a valuable technique for studying the thermal behavior and decomposition profiles of materials like CS and extracted chitin (Pemberton *et al.*, 2018). TGA curves provide critical information on the purity and thermal stability of chitin, helping researchers assess the effectiveness of various extraction methods and solvents in producing chitin with desired properties for applications in bioplastics, biomedicine, and agriculture (Pemberton *et al.*, 2018). The TGA curves of CS, AA-Ch, and chitin extracted using lactic-NADES are shown in Figure 6. In the TGA curve of CS (Figure 6a), gradual weight loss over the entire temperature range is observed. The initial weight loss at lower temperatures is attributed to the evaporation of adsorbed moisture and volatile organic compounds on the CS surface (Li *et al.*, 2023). As the temperature increases, further weight loss occurs due to the decomposition of organic components like proteins, lipids, and carbohydrates in the CS. Additionally, the presence of inorganic constituents, such as calcium carbonate from the CS's mineral content, may contribute to further weight loss at higher temperatures. The TGA curve of AA-Ch (Figure 6b) reveals that the higher purity chitin extracted through conventional acid/alkali

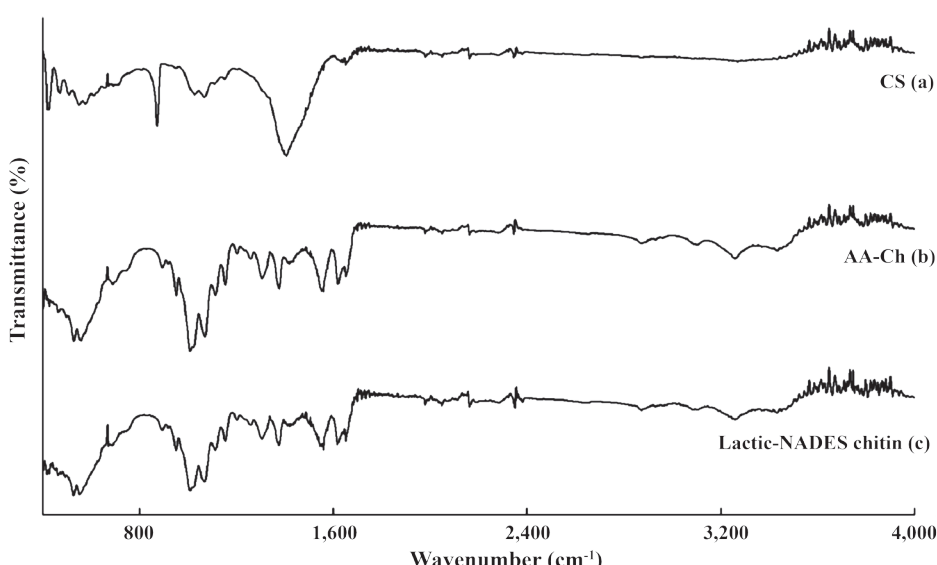


Figure 5. Figures showing FT-IR of: (a) crab shells powder (CS); (b) chitin extracted using acid/alkali (AA-Ch); and (c) chitin extracted using lactic-NADES (lactic-NADES chitin).

treatment exhibits reduced weight loss compared to CS. The initial weight loss due to moisture and volatile compounds is less prominent, indicating the effective removal of non-chitin components. The main weight loss in the TGA curve corresponds to the decomposition of chitin, which occurs at higher temperatures, typically above 200 °C. The TGA curve remains relatively stable until the onset of chitin decomposition, indicating the successful removal of non-chitin constituents during the extraction process. The TGA curve of chitin extracted using lactic-NADES (Figure 6c) is of particular interest due to the unique extraction method. Like AA-Ch, the TGA curve of chitin extracted via NADES displays higher purity with less initial weight loss compared to CS. The thermal decomposition of chitin occurs at temperatures similar to those observed for AA-Ch, indicating comparable thermal stability between chitin extracted by both methods. In a study by Pemberton *et al.* (2018), TGA was employed to analyze the thermal behavior of chitin extracted from CS using conventional acid/alkali treatment. The TGA curve

of chitin displayed a two-step weight loss pattern: the initial weight loss at lower temperatures (100–200 °C) due to the removal of moisture and other volatile components, followed by a second weight loss at higher temperatures (above 250 °C) corresponding to chitin decomposition. The study demonstrated that the conventional acid/alkali extraction effectively removed non-chitin constituents, resulting in a more thermally stable chitin product. In a comparative study by Li *et al.* (2023), TGA was used to compare the thermal stability of chitin extracted from CS using different methods, including conventional acid/alkali treatment and enzymatic extraction. The TGA curves revealed that chitin obtained through conventional acid/alkali treatment displayed a higher onset temperature for decomposition compared to enzymatically extracted chitin. The results suggested that the conventional acid/alkali method yielded chitin with enhanced thermal stability due to the removal of impurities. A study by Saravana *et al.* (2018) investigated the TGA thermograms of chitin extracted from CS using lactic-NADES. The TGA analysis revealed that

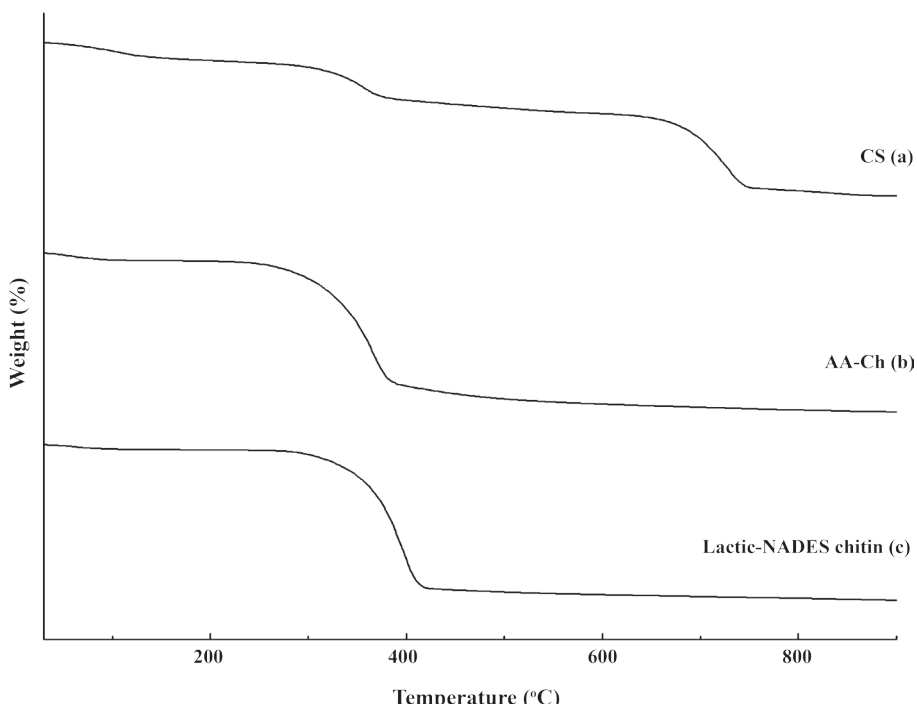


Figure 6. TGA curve of: (a) crab shells powder (CS); (b) chitin extracted using acid/alkali (AA-Ch); and (c) chitin extracted using lactic-NADES (lactic-NADES chitin).

lactic-NADES extracted chitin exhibited a weight loss profile similar to chitin extracted via conventional acid/alkali treatment. The TGA curves displayed a two-step decomposition pattern, with initial weight loss attributed to moisture and volatile compounds, followed by the decomposition of chitin at higher temperatures. The study indicated that the thermal stability of chitin extracted via lactic-NADES was comparable to that of chitin extracted through conventional acid/alkali method.

Further study by Saravana *et al.* (2018) and Li *et al.* (2023) explored the influence of different lactic-NADES compositions on the thermal behavior of chitin extracted from CS using TGA. The analysis revealed that the NADES composition significantly influenced the thermal stability of the extracted chitin. Specifically, the onset temperature of chitin decomposition varied with different NADES formulations, suggesting that the choice of NADES components can affect the thermal properties of the resulting chitin. Understanding the thermal behavior of chitin is crucial for optimizing extraction processes and tailoring chitin properties for specific applications, such as biodegradable materials and drug delivery systems.

CONCLUSIONS

In conclusion, this study highlights the superior demineralization and deproteinization efficiency of lactic-NADES compared to succinic-NADES in the chitin extraction process from crab shell waste. The optimization of chitin extraction with lactic-NADES, focusing on lactic acid concentrations and crab shell to lactic-NADES ratios, identified the optimal condition as a molar concentration of 3 M and a CS: lactic-NADES ratio of 1:20, with a microwave irradiation time of 5 min. This condition demonstrated a high demineralization efficiency of $97.78 \pm 0.73\%$ and deproteinization efficiency of $81.33 \pm 0.91\%$. SEM images revealed that lactic-NADES chitin exhibits a homogeneous fibrous or fibrillar structure, similar to AA-Ch. This observation suggests that chitin obtained through the NADES method maintains its structural

integrity and possesses similar morphological features to chitin extracted through the conventional acid-alkaline method. XRD analysis confirmed that lactic-NADES extracted chitin retained its crystalline nature, comparable to chitin obtained through conventional acid/alkali treatment. FT-IR results indicated that the lactic-NADES chitin structure closely resembles that of chitin obtained through acid/alkali treatment. Additionally, TGA demonstrated that the thermal stability of lactic-NADES extracted chitin is comparable to conventionally extracted chitin. These findings collectively highlight the efficiency and eco-friendliness of lactic-NADES as a promising approach for chitin extraction, holding significant implications for diverse applications in biotechnology, materials science, and other domains.

ACKNOWLEDGEMENT

The authors would like to thank Kasetsart University-Ocean University of China (KU-OUC) dual degree program for financial support.

LITERATURE CITED

Aranaz, I., M. Mengibar, R. Harris, I. Panos, B. Miralles, N. Acosta, G. Galed and A. Heras. 2009. Functional characterization of chitin and chitosan. **Current Chemical Biology** 3(2): 203–230. DOI: 10.2174/187231309788166415.

Dai, Y., J. van Spronsen, G.J. Witkamp, R. Verpoorte and Y.H. Choi. 2013a. Ionic liquids and deep eutectic solvents in natural products research: mixtures of solids as extraction solvents. **Journal of Natural Products** 76(11): 2162–2173. DOI: 10.1021/np40051w.

Dai, Y., J. van Spronsen, G.J. Witkamp, R. Verpoorte and Y.H. Choi. 2013b. Natural deep eutectic solvents as new potential media for green technology. **Analytica Chimica Acta** 766: 61–68. DOI: 10.1016/j.aca.2012.12.019.

de Queiroz Antonino, R., B.R.P. Lia Fook, V.A. de Oliveira Lima, R.I. de Farias Rached, E.P.N. Lima, R.J. da Silva Lima, C.O. Peniche Covas and M.V. Lia Fook. 2017. Preparation and characterization of chitosan obtained from shells of shrimp (*Litopenaeus vannamei* Boone). **Marine Drugs** 15(5): DOI: 10.3390/md15050141.

El Knidri, H., R. Belaabed, A. Addaou, A. Laajeb and A. Lahsini. 2018. Extraction, chemical modification and characterization of chitin and chitosan. **International Journal of Biological Macromolecules** 120: 1181–1189. DOI: 10.1016/j.ijbiomac.2018.08.139.

Gómez, A., A. Biswas, C. Tadini, R. Furtado, C. Alves and H. Cheng. 2019. Use of natural deep eutectic solvents for polymerization and polymer reactions. **Journal of the Brazilian Chemical Society** 30: 717–726. DOI: 10.21577/0103-5053.20190001.

Gomez, F.J.V., M. Espino, M.A. Fernández and M.F. Silva. 2018. A greener approach to prepare natural deep eutectic solvents. **ChemistrySelect** 3: 6122–6125. DOI: 10.1002/slct.201800713.

Gontrani, L., N.V. Plechkova and M. Bonomo. 2019. In-depth physico-chemical and structural investigation of a dicarboxylic acid/choline chloride natural deep eutectic solvent (NADES): A spotlight on the importance of a rigorous preparation procedure. **ACS Sustainable Chemistry and Engineering** 7(14): 12536–12543. DOI: 10.1021/acssuschemeng.9b02402.

Hamed, I., F. Özogul and J.M. Regenstein. 2016. Industrial applications of crustacean by-products (chitin, chitosan, and chitooligosaccharides): A review. **Trends in Food Science and Technology** 48: 40–50. DOI: 10.1016/j.tifs.2015.11.007.

Joseph, S.M., S. Krishnamoorthy, R. Paranthaman, J.A. Moses and C. Anandharamakrishnan. 2021. A review on source-specific chemistry, functionality, and applications of chitin and chitosan. **Carbohydrate Polymer Technologies and Applications** 2: 100036 DOI: 10.1016/j.carpta.2021.100036.

Kumari, S. and R. Kishor. 2020. **Chitin and chitosan**. In: Chitin and Chitosan: Origin, Properties, and Applications (eds. S. Gopi, S. Thomas and A. Pius), pp. 1–33. Elsevier, Bhopal, India.

Li, Z., M.C. Li, C. Liu, X. Liu, Y. Lu, G. Zhou, C. Liu and C. Mei. 2023. Microwave-assisted deep eutectic solvent extraction of chitin from crayfish shell wastes for 3D printable inks. **Industrial Crops and Products** 194: 116325. DOI: 10.1016/j.indcrop.2023.116325.

Liu, Y., J.B. Friesen, J.B. McAlpine, D.C. Lankin, S.N. Chen and G.F. Pauli. 2018. Natural deep eutectic solvents: Properties, applications, and perspectives. **Journal of Natural Products** 81(3): 679–690. DOI: 10.1021/acs.jnatprod.7b00945.

Margariti, C. 2019. The application of FTIR microspectroscopy in a non-invasive and non-destructive way to the study and conservation of mineralised excavated textiles. **Heritage Science** 7: 63. DOI: 10.1186/s40494-019-0304-8.

Ozel, N. and M. Elibol. 2021. A review on the potential uses of deep eutectic solvents in chitin and chitosan related processes. **Carbohydrate Polymers** 262: 117942. DOI: 10.1016/j.carbpol.2021.117942.

Pachapur, V.L., K. Guemiza, T. Rouissi, S.J. Sarma and S.K. Brar. 2016. Novel biological and chemical methods of chitin extraction from crustacean waste using saline water. **Journal of Chemical Technology and Biotechnology** 91: 2331–2339. DOI: 10.1002/jctb.4821.

Paiva, A., R. Craveiro, I. Aroso, M. Martins, R.L. Reis and A.R.C. Duarte. 2014. Natural deep eutectic solvents—Solvents for the 21st century. **ACS Sustainable Chemistry and Engineering** 2(5): 1063–1071. DOI: 10.1021/sc500096j.

Pedrol, N. and P. Tamayo. 2001. **Plant ecophysiology techniques**. In: Protein Content Quantification by Bradford Method (ed. M.J. Reigosa Roger), pp. 283–295. Kluwer Academic Publishers, Dordrecht, Netherlands.

Pemberton, A.T., D.B. Magers and D.A. King. 2018. Integrated TGA, FTIR, and computational laboratory experiment. **Journal of Chemical Education** 96(1): 132–136. DOI: 10.1021/acs.jchemed.8b00607.

Rahayu, A.P., A.F. Islami, E. Saputra, L. Sulmartiwi, A.U. Rahmah and K.A. Kurnia. 2022. The impact of the different types of acid solution on the extraction and adsorption performance of chitin from shrimp shell waste. **International Journal of Biological Macromolecules** 194: 843–850. DOI: 10.1016/j.ijbiomac.2021.11.137.

Santana, A.P.R., J.A. Mora-Vargas, T.G.S. Guimarães, C.D.B. Amaral, A. Oliveira and M.H. Gonzalez. 2019. Sustainable synthesis of natural deep eutectic solvents (NADES) by different methods. **Journal of Molecular Liquids** 293: 111452 DOI: 10.1016/j.molliq.2019.111452.

Saravana, P.S., T.C. Ho, S.J. Chae, Y.J. Cho, J.S. Park, H.J. Lee and B.S. Chun. 2018. Deep eutectic solvent-based extraction and fabrication of chitin films from crustacean waste. **Carbohydrate Polymers** 195: 622–630. DOI: 10.1016/j.carbpol.2018.05.018.

Saxena, R.K., S. Saran, J. Isar and R. Kaushik. 2017. **Production and applications of succinic acid.** In: Current Developments in Biotechnology and Bioengineering (eds. A. Pandey, S. Negi and C.R. Soccol), pp. 601–630. Elsevier, New delhi, India.

Shamshina, J.L., P. Berton and R.D. Rogers. 2019. Advances in functional chitin materials: A review. **ACS Sustainable Chemistry and Engineering** 7(7): 6444–6457. DOI: 10.1021/acssuschemeng.8b06372.

Tolesa, L.D., B.S. Gupta and M.J. Lee. 2019. Chitin and chitosan production from shrimp shells using ammonium-based ionic liquids. **International Journal of Biological Macromolecules** 130: 818–826. DOI: 10.1016/j.ijbiomac.2019.03.018.

Vanda, H., Y. Dai, E.G. Wilson, R. Verpoorte and Y.H. Choi. 2018. Green solvents from ionic liquids and deep eutectic solvents to natural deep eutectic solvents. **Comptes Rendus Chimie** 21(6): 628–638. DOI: 10.1016/j.crci.2018.04.002.

Vicente, F.A., M. Hus, B. Likozar and U. Novak. 2021. Chitin deacetylation using deep eutectic solvents: Ab initio-supported process optimization. **ACS Sustainable Chemistry and Engineering** 9(10): 3874–3886. DOI: 10.1021/acssuschemeng.0c08976.

Yang, Z. 2019. Natural deep eutectic solvents and their applications in biotechnology. **Advances in Biochemical Engineering/Biotechnology** 168: 31–59. DOI: 10.1007/10_2018_67.

Zhu, P., Z. Gu, S. Hong and H. Lian. 2017. One-pot production of chitin with high purity from lobster shells using choline chloride-malonic acid deep eutectic solvent. **Carbohydrate Polymers** 177: 217–223. DOI: 10.1016/j.carbpol.2017.09.001.